

A09s07

Heat storage for the coupling of Waste Heat Recovery and hydrogen production in a Solid-Oxide electrolyser

Titouan Fabiani (1, 2, 3), Patrice Tochon (1), Nolwenn Le Pierrès (2), Pierre Dumoulin (3)

(1) GENVIA SAS, Plaine Saint Pierre, 34500 Béziers/France;

(2) Univ Savoie Mont-Blanc, CNRS, LOCIE, 73370 Le Bourget-du-Lac/France;

(3) CEA, LITEN, DTCH, LCST, 38000 Grenoble/France;

Tel.: +33 4 38 78 44 30

titouan.fabiani@genvia.com

Abstract

Efficient operation of a Solid-oxide steam electrolyser requires a well-designed heat management system to heat the entering streams up to the electrolyser temperature (700-850°C). The nature of the heat input used to generate steam has indeed a strong impact on the hydrogen production overall efficiency. In this work, a thermal system is designed to produce steam from industrial waste heat. Exhaust industrial gases are recovered and sent to a tube bundle recuperator to heat a thermal oil loop (Figure A). Then, hot thermal oil is used in a plate SG to preheat liquid water and generate steam. Heat exchangers are eventually used to recover the heat of the electrolyser hot outlet streams. A thermocline sensible storage is added to the oil loop with the objective of maintaining a constant steam flowrate to the solid-oxide electrolyser despite the highly variable availability of industrial waste heat. The control of the whole thermal system is realized thanks to different pumps and valves in the oil loop and gas flow. The different components are dimensioned and modeled using Dymola software. The control strategy is studied and optimized to maintain a stable electrolyser operation.

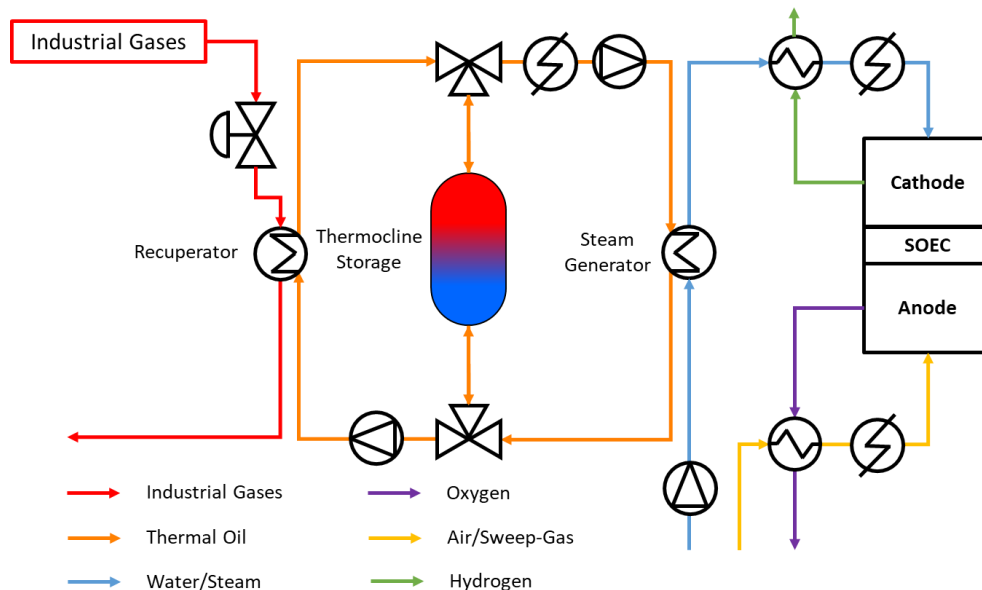


Figure A : Scheme of the proposed thermal system for the coupling of waste heat recovery, heat storage and steam generation for a Solid-Oxide steam electrolyser.



Introduction

Hydrogen is seen by numerous experts as a potential great energetic vector for future applications of mobility, district heating and long-term electricity storage. In this context, the SOEC (Solid Oxid Electrolysis Cell) technologies represent an option of great interest thanks to a higher electrical efficiency η_{elec}^{LHV,H_2} than the other electrolysis technologies, proton-exchange membrane (PEM) and alkaline (AEL). Indeed, when considering the Lower Heating Value (LHV) in the calculation, the efficiency η_{elec}^{LHV,H_2} of SOEC could reach more than 80% compared to between 60 and 70% for the other two technologies [1]. This gives the SOEC technologies a good potential for producing cheap hydrogen even in the case of high electricity costs [2].

These numerous advantages come with the complexity of operating an appliance at a high temperature $T_{cell} \in [700^\circ\text{C} ; 900^\circ\text{C}]$. Indeed, the stack needs to be maintained at T_{cell} and water needs to be evaporated and heated up to T_{cell} before entering the stack. Thus, the thermal management surrounding the stack has a critical impact on the final efficiency of the system. Petipas et al. [3] show that the electricity required to produce low-temperature steam represents 18% of the total electricity consumed in the system. Hence, an 18% difference between the efficiencies of two SOEC architectures could depend solely on the thermal management system chosen.

In this paper, the possibility of a thermal coupling of a SOEC with waste heat recovery (WHR) from industries is explored. The objective is the development of a thermal system for the generation of steam thanks to the recovery of industrial waste heat. When comparing the characteristics of the SOEC and WHR systems, their compatibility is far from obvious. On one hand, the WHR system thermal output can strongly vary and even be stopped. On the other hand, the operation of the SOEC system requires a constant steam generation rate at a constant pressure and temperature. For small resource variations, the utilization of complementary devices such as an electrical heater can help regulating the system. However, for large variations or for WHR shutdowns, planned or unplanned, these devices would not be sufficient.

Thermal energy storage (TES) systems are used in many thermal applications to avoid correspondence issues between the thermal energy supply and the heat demand. They avoid the loss of excess heat by storing it for later ([4], [5]). They also offer solutions for shutdowns by providing the previously stored energy. As shown in Figure 1, this work proposes to study the integration of a thermocline TES system in a steam generation system from WHR. In this architecture, exhaust industrial gases are recovered and sent to the recuperator to heat a thermal oil loop. Then, hot thermal oil is used in a SG (steam generator) to generate steam. High-temperature heat exchangers are then used to recover the heat of the electrolyser hot outlet streams. Eventually, the inlet streams are heated electrically to enter the SOEC at T_{cell} .

The thermocline TES and an additional electrical heater are integrated on the oil loop with the objective of maintaining a constant steam flowrate to the SOEC despite the highly variable availability of industrial waste heat. The control of the whole thermal system is realized thanks to different pumps and valves in the oil loop and gas flow. The objective is to generate a constant steam flowrate \dot{m}_w^{SG} in the SG. An additional objective is to maintain a constant temperature $T_{w,out}^{SG}$ of steam at the outlet of the SG to minimize the impact on the thermal components located after the SG.

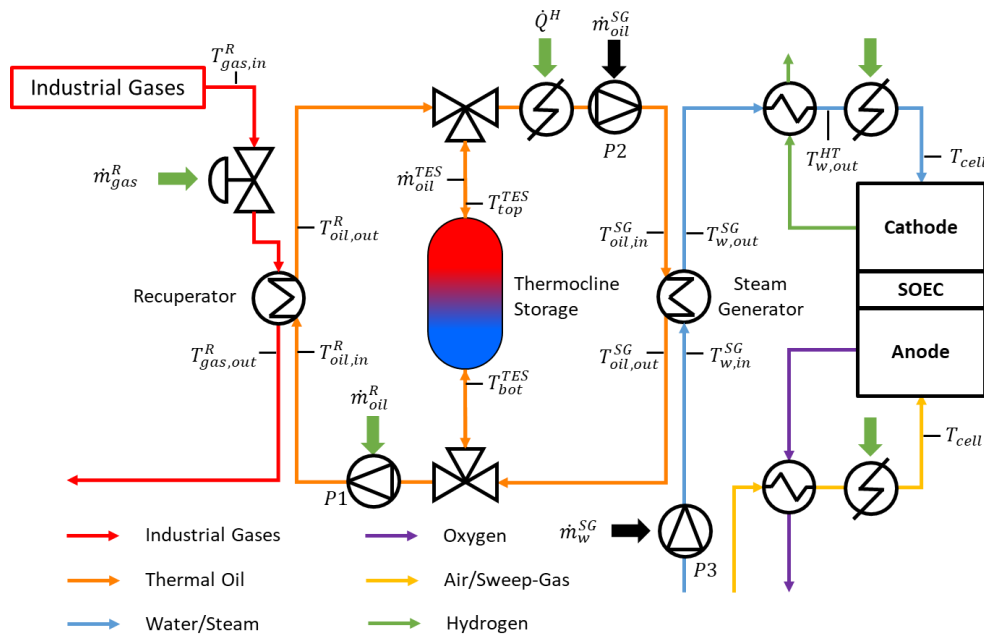


Figure 1 : Scheme of the proposed thermal system for the coupling of waste heat recovery, heat storage and steam generation for a Solid-Oxide steam electrolyser.

As shown by the green and black arrows in Figure 1, the control strategy must respect some constraints. The flow rate \dot{m}_w^{SG} of water sent in the SG must obviously be constant to produce a constant steam flow. In addition, to maintain a constant temperature of steam at the outlet of the SG, a constant amount of heat \dot{Q}_{ex}^{SG} must be exchanged in the SG. This can be assured by providing a constant flow rate \dot{m}_{oil}^{SG} of oil in the steam generator at a constant temperature $T_{oil,in}^{SG}$. As shown in Figure 1, pumps P2 and P3 are therefore operated in a stationary mode. The remaining components can be controlled to maintain the temperature of oil entering the SG. These components are : a valve controlling the gas flow \dot{m}_{gas}^R entering the recuperator ; a pump P1 upstream of the recuperator to control the oil flow rate \dot{m}_{oil}^R in the recuperator and an electrical heater upstream of the SG pump P2 to provide the heat \dot{Q}^H to the entering oil flow. The direction and value of the flow \dot{m}_{oil}^{TES} of thermal oil in the thermocline TES is then a consequence of the two other flows in the oil loop. It is considered positive in loading mode flowing downwards. Eventually, two heaters are located just upstream of the SOEC system to ensure that the inlet streams are at T_{cell} .

1. Scientific Approach

In the state of the art, the steam generation and thermal management of the SOEC systems are realized by electrical means. The main interest in developing such a thermal coupling with external heat sources is to replace part of the electrical power consumed by WHR thermal power. Of course, the recovery of this thermal power comes with the capital cost of installation of the different thermal and fluidics components and with their relatively small but yet existing electricity consumption. The objective of this work is therefore to evaluate the influence of installing such a thermal system on the final electricity consumption needed to produce a given amount of hydrogen. To do so, the system is simulated dynamically.

This whole SOEC system can be divided in two different sub-systems: the WHR-SG sub-system and the SOEC sub-system. The WHR-SG sub-system is composed of the thermal

components located at the left of the steam generator in Figure 1. This sub-system is characterized by a highly dynamic behavior because of the variations in the thermal power available from the industrial waste gases. Therefore, this sub-system is modeled using the Dymola software based on the Modelica language. This software is especially designed to simulate dynamic energy systems. The SOEC sub-system is composed of the SOEC system as well as the exchangers and heaters located downstream of the SG. On the contrary to the WHR-SG sub-system, the SOEC sub-system is, as much as possible, operated in stationary mode. Therefore, dynamic modeling and simulation are not necessary here. This sub-system is modeled using a Python program.

WHR-SG sub-system

The WHR-SG sub-system is composed of three main components: the recuperator, the thermocline TES and the steam generator.

Recuperator

The recuperator is designed to exchange heat between a gas and a liquid thermal oil. The exchanger technology chosen for this purpose is a bundle of tubes in a cross flow configuration. Since no phase change occurs in the recuperator, a LMTD model with the calculation of a global thermal resistance between the air and gas flow is used. A correction factor of 0.85 is considered to take into account the cross flow configuration. The thermal resistance on the gas and oil side are calculated respectively thanks to the correlation proposed by Zukauskas and Ulinskas [6] and the correlation proposed by Gnielinski [7]. The coefficient of heat transfer highly depends on the mass flow of fluid sent to the exchanger and the thermal resistances are hence evaluated at each time step.

Steam Generator

The SG is designed as a corrugated plate heat exchanger. There are three different zones in the SG: the preheating zone in which liquid water is heated from $T_{ambient} = 20^{\circ}C$ to its saturation temperature $T_{w,sat}$; the evaporation zone in which liquid water is evaporated at the constant temperature $T_{w,sat}$ and the superheating zone in which steam is heated from $T_{w,sat}$ to $T_{w,out}^{SG}$. Since the mass flows of oil and water are constant, the values of the heat transfer coefficients can also be considered constant. For the monophasic flows, the correlation from Focke et al. [8] is used. For the diphasic flow, a correlation proposed by the GRETh [9] is used. This correlation is obtained by taking the maximum value between a convective boiling and a nucleate boiling coefficients. The convective coefficient is obtained with the correlation from Focke et al. [8] and the nucleate boiling coefficient is obtained with the correlation developed by Cooper [10]. Hence, a global heat transfer coefficient is obtained for each zone. The behavior of the SG slightly varies depending on the inlet temperature of thermal oil. The parameters impacted are the length of the 3 zones inside the exchanger as well as the zones inlet and outlet temperatures. LMTD models are used on the preheating and evaporation zone to calculate the exchange area required by these two zones. Eventually, a third LMTD model is used to calculate the outlet temperature of steam based on the remaining exchange area.

TES system

For economic and practical considerations, the TES chosen is a 1-tank dual-media sensible storage system. Both the hot and cold volumes thermal oil are stored in the same tank. The hot fluid is naturally stored above the cold fluid due to differences in density. Loading and unloading of the tank are realized by, respectively, injecting or retrieving hot fluid at the top of the tank. The tepid zone between the cold and hot volumes of thermal oil is called “thermocline”. Efficient operation of a 1-tank thermocline TES system aims at preventing the tepid zone to extend, thus preserving the energetic value of the stored hot fluid. Figure 2 shows a scheme of a thermocline TES system and a diagram of the physical phenomena represented in the model used in this work.

The TES system is a cylinder with dome roofs at its top and bottom. Thermal oil being very expensive, part of the tank is filled with rocks. Loading of the TES is realized by the exchange of heat between the thermal oil and the rock bed. When the flow velocity u inside the TES is below 3 mm/s [11], the flow behaves like a piston flow and there are few recirculation flows. This prevents significant mixing between the hot and cold zones, which would be detrimental to the TES operation. In this case, the temperature differences are small over a cross-section and the behavior of the TES system can be modeled in 1-D.

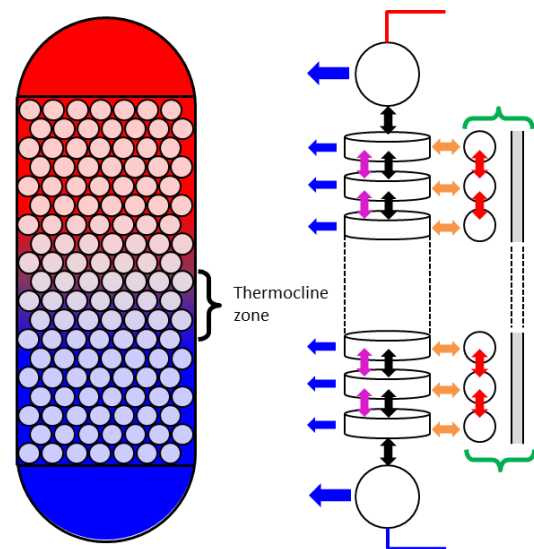


Figure 2: Diagram of the physical phenomena represented in the model of thermocline TES system.

In this study, the TES system is thus discretized in 1-D along its vertical axis in the rock bed according to the method of finite volumes with 40 meshes. The model considered is based on a previous work by Esence et al. [11]. Figure 2 presents the physical phenomena represented in the model. At each height, a finite volume is considered for thermal oil with the solving of both the energy and mass conservation equations. Also, a finite volume is considered for the solid with the solving of the energy conservation equation. The following phenomena are taken into account: oil mass transfer along the vertical axis (in black in Figure 2); conducto-convective heat exchange between the oil and the rock (in orange); heat diffusion along the vertical axis in the oil (in pink); conduction along the vertical axis in the rock bed (in red) and thermal losses through the wall and the dome roofs (in blue). The vertical conductivity as well as the thermal inertia of the walls is considered via effective terms in the energy conservation equation of the rock matrix (represented by green braces in Figure 2). A layer of insulation surrounding the tank is also considered.

Other components

The other components of the WHR-SG sub-system are the following: a butterfly valve for the regulation of the gas flow, two pumps P1 and P2 for the control of the flow in the oil loop, an electric heater on the oil loop and one water pump P3 upstream of the SG. The electric heater is discretized along the flow axis with the thermal inertia of the wall considered.

SOEC sub-system

The SOEC sub-system is composed of the high-temperature exchangers and heaters located downstream of the SG and the SOEC itself. The SOEC is modeled as a black box. Every molecule of steam generated by the SG is eventually transformed into a molecule of dihydrogen. Therefore, we can consider the following formula: $\dot{m}_{H_2}^{prod} = \frac{\dot{m}_{w,out}^{SG}}{9}$ based on the ratio between their molar masses. Also, for the electricity consumption of the SOEC system, we consider the value of $P_{elec} = 39 \text{ kWh/kg}_{H_2}$ as given by the SRIA 2021-2027 report of the European Union Clean Hydrogen Joint Undertaking [12]. This value represents a 2024 European objective to produce hydrogen at atmospheric pressure by SOEC.

The high-temperature exchangers are modeled with a constant efficiency of 0.9 and their modeling is only realized to see if the variations in steam temperature at the outlet of the SG have an impact on the electricity consumption of the high-temperature heaters. The heaters are represented by an electricity consumption equal to their thermal output.

Sizing of the system

The thermal system is designed based on the choice of a hot $T_{oil,hot}$ and a cold $T_{oil,cold}$ temperatures for the oil loop. $T_{oil,hot}$ is chosen thanks to a pinch analysis of the recuperator after a study of the industrial gases temperature data. For 80% of the dataset, the gas inlet temperature is higher than 200°C. $T_{oil,hot}$ is therefore chosen as 185°C to ensure a 15 K temperature difference between oil and gas along the recuperator. A possible variation of +/- 5 K is considered on $T_{oil,hot}$ and the SG is dimensioned on the most restrictive case for $T_{oil,in}^{SG} = 180^\circ\text{C}$. $T_{oil,cold}$ is chosen based on a pinch analysis of the SG. In the SG, the pinch is located between the saturation temperature of water and the corresponding oil temperature at the beginning of steam generation. Steam generation is realised at the pressure $P_{cell} = 1.6 \text{ bar}$ which corresponds to a saturation temperature $T_{sat} = 112.3^\circ\text{C}$. Here again, a 15 K temperature pinch is chosen which means that oil must be at 130°C at the beginning of steam generation. In the end, we obtain $T_{oil,cold} = 120^\circ\text{C}$. Based on the thermodynamic characteristics of oil and water, we obtain a factor of 22.2 between the water and oil mass flow to have $\dot{m}_{oil}^{SG} * (180 - 130) = \dot{m}_w^{SG} * h_{lv,w}$ with $h_{lv,w}$ the latent heat of vaporization of water.

The sizing of the plate SG is realized based on these temperature and mass flow values. For the recuperator, the hot and cold oil temperatures $T_{oil,hot}$ and $T_{oil,cold}$ are considered on the oil side and the exchanger is dimensioned based on the mean values of mass flow rate and temperature of industrial gases. The thermozone cross-section is chosen to keep the flow velocity u below 3 mm/s when the oil mass flow exiting the TES is equal to the oil mass flow sent to the SG: $\dot{m}_{oil}^{TES} = -\dot{m}_{oil}^{SG}$ (unloading mode). In the first sizing, the thermozone system is sized to store the energy corresponding to 3,2 hours of steam generation. Eventually, the oil loop electric heater is dimensioned to be able to generate steam even if no heat is available in the recuperator or in the TES. Therefore, the heater is dimensioned to heat an oil mass flow \dot{m}_{oil}^{SG} from $T_{oil,cold}$ to $T_{oil,hot}$.

2. Simulations

The input dataset represents the variations in temperature and flowrate of a typical industrial waste heat resource for 5 hours. This industrial waste heat takes the form of industrial gases. During the 5-hour period, the plant operation is continuous. The response of the WHR-SG subsystem to the variations of this dataset are simulated on Dymola to obtain the system electricity consumption as well as the temperature and mass flow rate of the steam output. The WHR-SG sub-system is operated according to an optimized control strategy.

Control strategy

The objective of the control strategy is to constantly provide an oil mass flow \dot{m}_{oil}^{SG} at $T_{oil,hot}$ at the entry of the SG with the lowest possible electricity consumption. To do so, it is possible to act on three different elements: the gas flow in the recuperator, the oil flow in the recuperator and the thermal power provided by the electric heater. For each of these elements a PID control loop is developed and added to the system. For the mass flows, the setpoint signal is $T_{oil,hot} = 185^{\circ}C$ and the measure signal is $T_{oil,out}^R$. For the heater, a temperature sensor at the inlet of P2 gives the measure signal. The heater PID control loop is operated independently to the other two elements to ensure that $T_{oil,in}^{SG}$ is always higher than $180^{\circ}C$. Hence, it is used either to compensate the temperature variations of $T_{oil,in}^{SG}$ or to heat the oil flow rate when no heat is available from the recuperator and the TES.

The right setpoint values for the three elements are decided based on the following system indicators: the recoverable power from the gas flow \dot{Q}_{reco}^R , and the temperatures at the bottom and at the top of the TES system T_{bot}^{TES} and T_{top}^{TES} . If \dot{Q}_{reco}^R is higher than the power exchanged at the SG \dot{Q}_{ex}^{SG} , the excess recovered heat $\dot{Q}_{excess}^R = \dot{Q}_{reco}^R - \dot{Q}_{ex}^{SG}$ is positive and it is stored in the TES. If $\dot{Q}_{reco}^R < \dot{Q}_{ex}^{SG}$, \dot{Q}_{excess}^R is negative and heat is retrieved from the TES. In both cases, the TES mass flow rate is the difference between the recuperator and SG mass flow rates : $\dot{m}_{oil}^{TES} = \dot{m}_{oil,PID}^R - \dot{m}_{oil}^{SG}$.

In nominal operation, the gas mass flow rate is the recoverable gas flow : $\dot{m}_{gas}^R = \dot{m}_{gas,reco}^R$ and the oil mass flow rate is controlled by the PID control loop on pump P1 : $\dot{m}_{oil}^R = \dot{m}_{oil,PID}^R$. The PID control loop ensures that $T_{oil,out}^R = T_{oil,hot}$. The WHR-SG subsystem is in nominal operation as long as $\dot{m}_{oil,PID}^R$ remains in $[\dot{m}_{oil,max}^R; \dot{m}_{oil,min}^R]$. To keep the TES flow velocity u below 3 mm/s during loading, we need to have $\dot{m}_{oil}^{TES} \leq \dot{m}_{oil}^{SG}$ in the TES, therefore $\dot{m}_{oil,max}^R = 2 * \dot{m}_{oil}^{SG} * \dot{m}_{oil,min}^R$ is the lowest mass flow rate for which the recuperator oil output temperature $T_{oil,out}^R$ can be controlled. Indeed, when the oil flow in the recuperator becomes laminar, the heat exchange becomes less efficient, and it is not possible anymore to control efficiently the output temperature. When $\dot{m}_{oil,PID}^R$ is outside $[\dot{m}_{oil,max}^R; \dot{m}_{oil,min}^R]$, \dot{m}_{oil}^R is set to its maximum or minimum value and the gas mass flow rate is controlled by the PID control loop on the valve: $\dot{m}_{gas}^R = \dot{m}_{gas,PID}^R$. Here again, it is operated to have $T_{oil,out}^R = T_{oil,hot}$. Eventually, when $T_{gas,in}^R < T_{oil,hot}$, both the oil and gas mass flow rates in the recuperator are set to zero. No heat is recovered in this case.

The control strategy is partially modified when the TES system is either completely loaded or unloaded. When it becomes completely unloaded, the thermocline zone reaches the top of the system and the oil temperature at the top starts to diminish. When $T_{top}^{TES} < T_{oil,cold}$, no

more heat can be recovered from the TES system and its oil mass flow \dot{m}_{oil}^{TES} is set to zero instead of negative when $\dot{Q}_{reco}^R < \dot{Q}_{ex}^{SG}$. Therefore, in these cases, the value of $\dot{m}_{oil,min}^R$ is set to \dot{m}_{oil}^{SG} and the temperature limit for recovering heat at the recuperator is lowered from $T_{oil,hot}$ to 130°C. Indeed, the objective becomes to heat the oil mass flow rate \dot{m}_{oil}^R by recovering as much heat as possible. When the TES is completely loaded, the excess recovered heat \dot{Q}_{excess}^R is only necessary to maintain the TES system loaded by compensating the heat losses. Therefore, in this situation, the maximum thermal power exchanged at the recuperator $\dot{Q}_{ex,max}^R$ is the thermal power necessary to heat a mass flow $\dot{m}_{oil,max}^R = \dot{m}_{oil}^{SG} + \dot{m}_{oil,HL}^{TES}$ from $T_{oil,cold}$ to $T_{oil,hot}$ with $\dot{m}_{oil,HL}^{TES}$, the mass flow necessary to compensate heat losses.

3. Results

Figure 3 shows the evolution of the WHR-SG sub-system key variables during a 5-hour simulation. During this period, the gas inlet temperature varies between 160°C and 500°C as can be seen in Figure 3.a), and the gas inlet mass flowrate (black) varies between 20 and 40 kg/s as presented in Figure 3.b). In Figure 3.a), the evolution of the recuperator oil mass flow rate \dot{m}_{oil}^R is presented in orange and it is compared to its maximum (black) and minimum value (green). In Figure 3.b), the evolution of the recuperator gas mass flow rate \dot{m}_{gas}^R is presented in red and it is compared to the recoverable gas flow $\dot{m}_{gas,reco}^R$ (black). Figures 3.c) and 3.d) present the evolution of the temperatures at the hottest point in, respectively, the recuperator and the SG. Figure 3.e) presents the evolution of the TES state of energy (SOE) which is equal to 0 when all the TES fluid and solid are at $T_{oil,cold}$ and 1 when they are at $T_{oil,hot}$. Eventually, Figure 3.f) represents the power exchanged at the recuperator (red) and at the SG (blue) and the power provided by the heater (black).

The operation of the control strategy can be seen in Figure 3). In the time slot [1h ; 2h], the system is in nominal operation. As can be seen in Figure 3.b), the gas flow is not regulated, and it is therefore equal to the recoverable gas flow $\dot{m}_{gas,reco}^R$. The oil mass flow rate is regulated by the PID controller (Figure 3.a)), and its value is between $\dot{m}_{oil,min}^R$ and $\dot{m}_{oil,max}^R$. The TES mass flow rate is then $\dot{m}_{oil}^{TES} = \dot{m}_{oil,PID}^R - \dot{m}_{oil}^{SG}$ and the thermal power loaded or unloaded is the excess recovered heat $\dot{Q}_{excess}^R = \dot{Q}_{reco}^R - \dot{Q}_{ex}^{SG}$. In the time slot [1h ; 1.5h], $\dot{Q}_{excess}^R < 0$ and the SOE slowly diminishes (Figure 3.e)). In the time slot [1.5h ; 2h], $\dot{Q}_{excess}^R > 0$ and the SOE increases.

In the time slot [2.1h ; 2.3h], the recoverable power \dot{Q}_{reco}^R is too high and $\dot{m}_{oil,PID}^R > \dot{m}_{oil,min}^R$. During this period, \dot{m}_{oil}^R is set to $\dot{m}_{oil,max}^R$ (Figure 3.a)) and the gas mass flow rate is regulated by a PID controller therefore $\dot{m}_{gas}^R < \dot{m}_{gas,reco}^R$ (Figure 3.b)). In the short time slots [2.5h ; 2.6h] and [2.9h ; 3.0], the recoverable power \dot{Q}_{reco}^R is too low and \dot{m}_{oil}^R is set to $\dot{m}_{oil,min}^R$. The gas mass flow rate is regulated by the PID controller. Eventually, when the gas flow temperature gets below $T_{oil,hot}$ in the time slot [2.6h; 2.9h], \dot{m}_{oil}^R and \dot{m}_{gas}^R are set to zero. No heat is exchanged in the recuperator and the TES mass flow is equal to the recuperator oil mass flow $\dot{m}_{oil}^{TES} = -\dot{m}_{oil}^{SG}$.

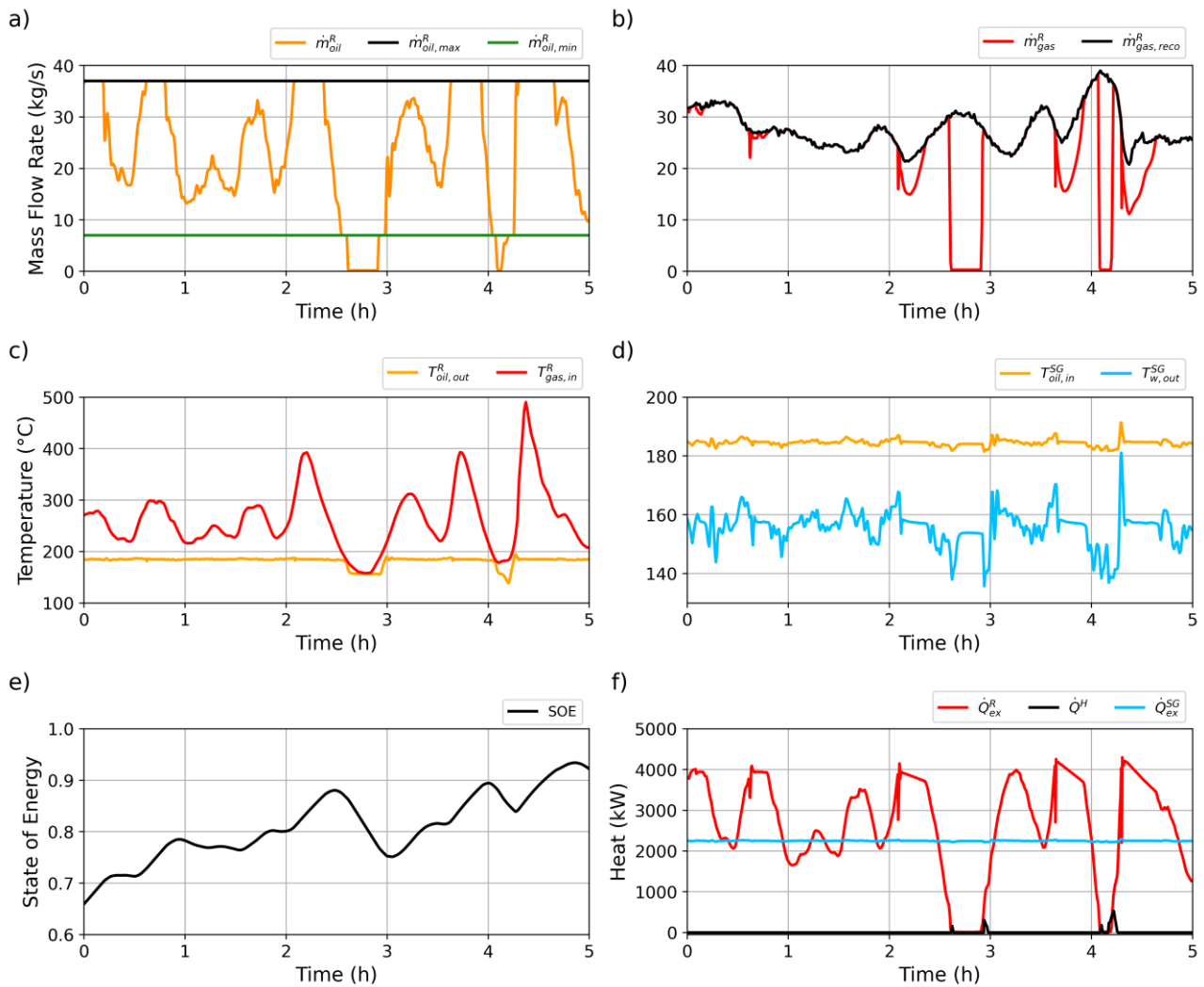


Figure 3: Evolution of the key variables in the thermal system : a) Oil mass flow rate in the recuperator ; b) Gas mass flow rate in the recuperator ; c) Temperatures at the hottest point of the recuperator ; d) Temperatures at the hottest point of the SG ; e) State of Energy (SOE) in the TES ; f) Thermal power exchanged at the recuperator and evaporator and power provided by the heater.

With this control strategy, the SG inlet temperature $T_{oil,in}^{SG}$ of oil is maintained between 180 and 192°C (see Figure 3.d). These little variations still have a strong impact on the steam outlet temperature $T_{w,out}^{SG}$. The latter varies between 135 and 180°C during the 5-hour simulation. To study the impact of these variations on the SOEC sub-system we simulate the response of the high-temperature steam-hydrogen heat exchanger. The steam temperature at the outlet of the system is shown in Figure 4. The exchanger has a smoothing effect on the temperature, which only varies between 600 and 610°C. This smoothing effect validates the scientific approach considered in this work which is to focus the study on the WHR-SG subsystem. The control strategy is optimized in the sense that when the TES system is not completely discharged, the electric heater is almost never used. In Figure 3.f), it only serves briefly to compensate the strong variations in power exchanged at $t=2.6h$, $t=2.9h$, $t=4.1h$ and $t=4.2h$.

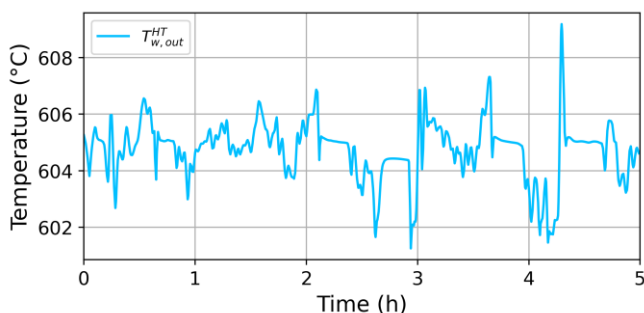


Figure 4: Temperature variations for the steam flow at the outlet of the high-temperature heat exchanger.

completely discharged, the electric heater is almost never used. In Figure 3.f), it only serves briefly to compensate the strong variations in power exchanged at $t=2.6h$, $t=2.9h$, $t=4.1h$ and $t=4.2h$.

Electrical energy savings

The operation of the WHR-SG subsystem is then simulated on a 13-day dataset to estimate the potential electrical energy savings. On this dataset, the operation of the plant is continuous. The total electrical energy consumption of three different architectures are compared and presented in Figure 5.a). These architectures are: A) steam is only generated thanks to an electrical heater, B) a WHR-SG subsystem without a TES is operated and C) a WHR-SG subsystem with a TES is operated. The electrical energy consumption (EEC) of system A) is about $46 \text{ kWh}/\text{kg}_{\text{H}_2,\text{prod}}$. The EEC of system B) and C) are respectively 87.2% and 85.7% of the EEC of system A). The thermocline TES system considered for system C) is big enough to generate steam without WHR for 3.2 hours. For a production of $1000 \text{ kg}_{\text{H}_2}/\text{day}$, the volume of such a TES would be about 30 m^3 and its energy capacity would be about 1000 kWh .

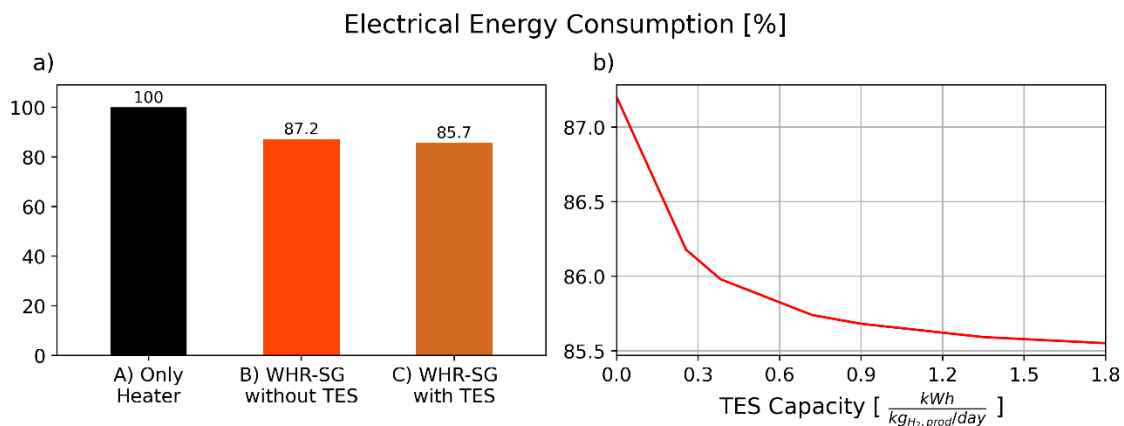


Figure 5 : Electrical energy consumption of the whole SOEC system : a) Comparison between three different architectures ; b) Consumption of the system with TES depending of the TES capacity.

Figure 5.b) shows the evolution of the system electrical energy consumption as a function of the TES energy capacity. In economic terms, reducing the system EEC and operational expenses (OPEX) is done thanks to an increase in the TES capacity installed and capital expenses (CAPEX). With a TES capacity of $0.9 \text{ kWh} \cdot \text{kg}_{\text{H}_2}^{-1} \cdot \text{day}^{-1}$ the EEC of the system is already reduced by 1.5% in comparison with a scenario without TES. As the TES gets oversized for the system, the rate of reduction in EEC is diminished. Indeed, at $1.8 \text{ kWh} \cdot \text{kg}_{\text{H}_2}^{-1} \cdot \text{day}^{-1}$, the EEC is only reduced by an additional 0.2% showing that the increase in the TES capacity is not so interesting anymore. These numeric results are strongly linked to the amplitude and frequency of the variations of \dot{Q}_{reco}^R in our dataset and cannot be generalised to other WHR resources. However, the general shape of the curve shown in Figure 5.b) should also be found in similar WHR-SG-TES thermal systems coupled to an SOEC. The shape of the curve suggests that an economic compromise can be found between the OPEX and CAPEX.

In comparison with a SOEC system working only with an electrical heater for SG, the coupling with a WHR-SG subsystem including a TES can save up to 15% in terms of EEC. This result is coherent with the ones observed by Petipas et al. [3] and demonstrates the optimal sizing of the thermal components and design of the control strategy. The comparison with literature is however limited by the differences in the SOEC models considered.

Future developments should include a techno-economic study as well as a study of the impact of different key parameters on the EEC and efficiency η_{elec}^{LHV,H_2} . Some of these key parameters include characteristics of the WHR resource considered, for instance the mean temperature of the waste gases, amplitude and frequency of the variations, potential production shutdown and a ratio between \dot{Q}_{reco}^R and \dot{Q}_{ex}^{SG} . The impact of the TES size in different configurations should also be explored.

References

- [1] S. A. Grigoriev, V. N. Fateev, D. G. Bessarabov, et P. Millet, « Current status, research trends, and challenges in water electrolysis science and technology », *International Journal of Hydrogen Energy*, vol. 45, n° 49, p. 26036-26058, oct. 2020, doi: 10.1016/j.ijhydene.2020.03.109.
- [2] M. Reytier *et al.*, « Stack performances in high temperature steam electrolysis and co-electrolysis », *International Journal of Hydrogen Energy*, vol. 40, n° 35, p. 11370-11377, sept. 2015, doi: 10.1016/j.ijhydene.2015.04.085.
- [3] F. Petipas, A. Brisse, et C. Bouallou, « Benefits of external heat sources for high temperature electrolyser systems », *International Journal of Hydrogen Energy*, vol. 39, n° 11, p. 5505-5513, avr. 2014, doi: 10.1016/j.ijhydene.2014.01.179.
- [4] G. Alva, Y. Lin, et G. Fang, « An overview of thermal energy storage systems », *Energy*, vol. 144, p. 341-378, févr. 2018, doi: 10.1016/j.energy.2017.12.037.
- [5] A. Gil *et al.*, « State of the art on high temperature thermal energy storage for power generation. Part 1—Concepts, materials and modellization », *Renewable and Sustainable Energy Reviews*, vol. 14, n° 1, p. 31-55, janv. 2010, doi: 10.1016/j.rser.2009.07.035.
- [6] A. Zukauskas et R. Ulinskas, « Heat transfer in tube banks in crossflow », janv. 1988, Consulté le: 2 mai 2024. [En ligne]. Disponible sur: <https://www.osti.gov/biblio/5833318>
- [7] V. Gnielinski, « New Equations for Heat and Mass Transfer in Turbulent Pipe and Channel Flow », *International Chemical Engineering*, vol. 16, n° 2, p. 359-368, 1976.
- [8] W. W. Focke, J. Zachariades, et I. Olivier, « The effect of the corrugation inclination angle on the thermohydraulic performance of plate heat exchangers », *International Journal of Heat and Mass Transfer*, vol. 28, n° 8, p. 1469-1479, août 1985, doi: 10.1016/0017-9310(85)90249-2.
- [9] GRETh, « e-Book », GRETh. Consulté le: 29 juin 2022. [En ligne]. Disponible sur: <https://greth.fr/e-book/>
- [10] M. G. Cooper, « SATURATION NUCLEATE POOL BOILING - A SIMPLE CORRELATION », in *First U.K. National Conference on Heat Transfer*, Elsevier, 1984, p. 785-793. doi: 10.1016/B978-0-85295-175-0.50013-8.
- [11] T. Esence, A. Bruch, J.-F. Fourmigué, et B. Stutz, « A versatile one-dimensional numerical model for packed-bed heat storage systems », *Renewable Energy*, vol. 133, p. 190-204, avr. 2019, doi: 10.1016/j.renene.2018.10.012.
- [12] Clean Hydrogen Joint Undertaking, « Clean Hydrogen JU - Strategic Research and Innovation Agenda 2021 – 2027 ». Consulté le: 8 décembre 2023. [En ligne]. Disponible sur: <https://www.clean-hydrogen.europa.eu/system/files/2022-02/Clean%20Hydrogen%20JU%20SRIA%20-%20approved%20by%20GB%20-%20clean%20for%20publication%20%28ID%2013246486%29.pdf>

Keywords: EFCF2024, Solid Oxide Technologies, SOC, Electrolysers, SOE, Heat Integration, Waste Heat Recovery, Heat Storage